Materials Science for Energy Technologies 3 (2020) 472–481

Contents lists available at ScienceDirect

Materials Science for Energy Technologies

journal homepage: www.keaipublishing.com/en/journals/materials-science-for-energy-technologies

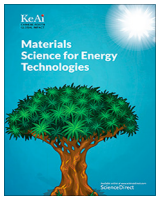

Functionalized metal oxide nanoparticles for efficient dye-sensitized solar cells (DSSCs): A review

D. Kishore Kumar [a,b,*], Jan Kříž [a], N. Bennett [b], Baixin Chen [b], H. Upadhayaya [c], Kakarla Raghava Reddy [d], Veera Sadhu [e,*]

[a] Department of Physics, University of Hradec Králové, Rokitanského 62, 500 03 Hradec Králové, Czech Republic
[b] Energy Conversion Lab (ECL), Institute of Mechanical Process and Energy Engineering (IMPEE), School of Engineering and Physical Sciences, Heriot-Watt University, Riccarton, Edinburgh EH14 4AS, UK
[c] Advanced Materials Centre, School of Engineering, London South Bank University, 103, Borough Road, London SE10AA, UK
[d] School of Chemical and Biomolecular Engineering, The University of Sydney, Sydney, NSW 2006, Australia
[e] School of Physical Sciences, Kakatiya Institute of Technology & Science (KITS), Warangal, Telangana 506015, India

ARTICLE INFO

Article history:
Received 5 January 2020
Revised 15 March 2020
Accepted 16 March 2020
Available online 25 March 2020

Keywords:
Dye-sensitized solar cells (DSSCs)
Photovoltaics
Semiconducting metal oxides
Quantum dots
Sensitizers
DSSC-device parameters

ABSTRACT

Dye-sensitized solar cells (DSSCs) are a next-generation photovoltaic energy conversion technology due to their low cost, ability to fabrication on various substrates, structural modifications, excellent transparency, photovoltaic output and its potential applications in wearable devices, energy sustainable buildings, solar-powered windows, etc. DSSC working devices consist of components such as conductive oxide substrates, photoanodes with wide bandgap semiconductors, dye molecules (sensitizers), counter electrodes and redox electrolytes, etc. High-efficiency DSSC devices can be fabricated suitable functionalization of semiconducting metal oxides with quantum dots, organic conjugated polymers, etc. In this review, we discuss different photovoltaic technologies, working principles of DSSCs, fabrication process of devices using various novel inorganic nanostructured materials, influencing parameters on the performance of DSC-device such as photoconversion efficiency (PCE), short circuit current (Jsc), open-circuit voltage (V_{oc}) and fill factor (FF).

Contents

* Corresponding authors at: Department of Physics, University of Hradec Králové, Rokitanského 62, 500 03 Hradec Králové, Czech Republic (D. Kishore Kumar).
E-mail addresses: nanokishore@gmail.com (D. Kishore Kumar), reddy.chem@gmail.com (K.R. Reddy), veera.sadhu@gmail.com (V. Sadhu).

Peer review under responsibility of KeAi Communications Co., Ltd.

https://doi.org/10.1016/j.mset.2020.03.003

1. Introduction

For any nation, the availability of resources such as minerals and fossil fuels, especially oil and gas is the backbone for economic growth and prosperity. As the population increases, the demand for energy also increases simultaneously. The Gulf War and oil crisis in the past and the scarcity of fossil fuels forced mankind to pay attention to clean energy resources. The quest for cheap and clean energy progressed towards revisiting the renewable sources. Wind, geothermal, hydro and solar energy are there presentative sources of renewable energy. Whereas wind power, geothermal and hydropower can be limited on geographical grounds, solar energy is the most available source on earth. The Earth receives about 174 (10^3 TW of solar radiation per year, whereas the total global energy consumption in one year is 15 TW (15 TW = 80 min) [1]. The tapping of Sun's radiation to a considerable amount will fulfill most of world's energy needs. The salient features of solar energy are:

(i) Solar energy is an almost everlasting renewable energy source [Sun = Billions of years].
(ii) Solar energy is free and all territories have equal rights to it without any major geographical differences.
(iii) Smart energy networks can be developed to use solar energy by incorporating emerging concepts like smart grid, minigrid conveniently allowing generation, demand, and supply.
(iv) The cost of the solar modules is decreasing sharply every year and the trend is expected to continue.
(v) Very low operating and maintenance cost for photovoltaic modules compared to the other renewable energy sources makes it simpler to install and operates without emission of any toxic gases.

The working principle of all photovoltaic devices and semiconductors devices are based on the photoelectric effect. The extensive research into photovoltaic (PV) effect since then has led to three generations of solar cells. The first-generation solar cells comprised of silicon solar cells and second-generation solar cells are also known as thin-film solar cells [2].

The theoretical photoconversion efficiency limit of these single-junction devices is about 33% which is based on the Shockley-Queisser limit which is nearly one third as compared to the Carnot limit of conversion of sunlight to electricity at 95% [3]. The third generation or emerging solar cells are based on different concepts such as up/down conversion, multiple exciton generation, multi-junction, hot carrier collections. Emerging solar cells are comprised of bulk heterojunction (BHJ); photoelectrochemical cells (PEC); dye-sensitized solar cells (DSSC); quantum dot sensitized solar cells (QDSSC) and perovskite solar cells. In 1991, the DSSC concept was first invented by Brian O'Regan and Michael Gratzel using mesoporous TiO_2 nanoparticles and ruthenium dye [4], and best photoconversion efficiency of DSSC is 14.3% [5].

This review describes different photovoltaic technologies, working principles, a fabrication process of devices using various novel inorganic nanostructured materials, influencing parameters on the performance of DSSC-device such as photoconversion efficiency (PCE), short circuit current (Jsc), open-circuit voltage (V_{oc}) and fill factor (FF).

2. History and current research in photovoltaics

The silicon solar cells have low maintenance costs and low operation costs but high manufacturing costs restrict the widespread of photovoltaic technology [6]. For commercial applications, either need to improve the photoconversion efficiencies or manufacturing costs should be lowered and present research is based on these facts.

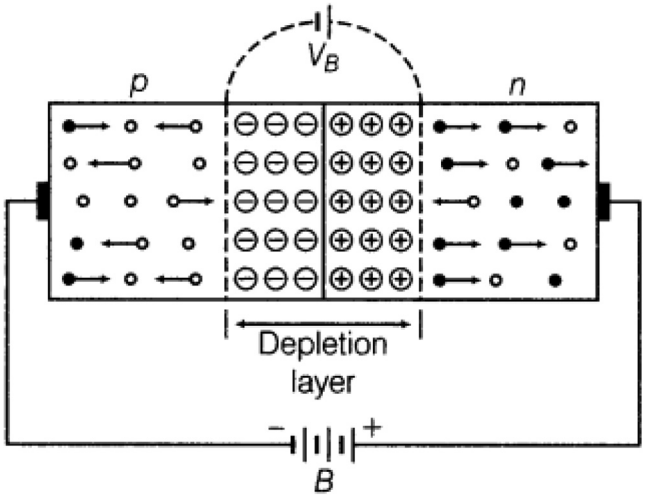

Fig. 1. Schematic representation of p-n junction diode. Reproduced withpermission from Ref. [8].

2.1. First-generation

First-generation solar cells consist of both crystalline and polycrystalline silicon solar cells are considered. More than half a century, these silicon solar cells are the dominant technology and account for nearly 90% share of the photovoltaic energy [7]. The top surface of crystalline silicon (c-Si) solar cells is doped with phosphorus by diffusion (Fig. 1).

The contacts are made by the screen printing method to the rear and fron of the cell. The best photoconversion efficiency (PCE) of silicon solar cells is only about 25% on the lab scale, whereas, PCE of commercial silicon cells is about 22% [9]. Preparation of high purity 99.9999% precursors are required in the fabrication of c-Si solar cells and this process is expensive and laborious [10]. This process adds directly to the manufacturing plant capital cost and photovoltaic modules [11]. The cost factor is inhibiting the widespread applications of silicon solar cells in electricity production. Higher efficiencies and carrier mobility with broad spectral absorption range are the major advantages of silicon solar cells [12,13]. Manufacturing cost is a major disadvantage for silicon solar cells [14]. The energy of photons generated at short wavelengths is wasted as heat. The energy payback period (EPP) associated with this technology is around 2–3 years [15].

2.2. Second generation/thin-film solar cells

Copper indium gallium diselenide (CIGS), cadmium telluride (CdTe), copper zinc tin sulphide (CZTS), amorphous silicon (a-Si) and thin-film crystalline silicon are categorized into thin-film solar cells. In thin-film solar cells, the photoactive material is prepared using thin-film techniques onto the glass or a flexible substrate. Hence these devices are termed as thin-film solar cells. In contrary to first-generation solar cells, second-generation solar cells offer low manufacturing cost, less material required and large area deposition. As direct bandgap photoactive materials have a high absorption coefficient, they require photoactive material of thickness less than a micron to absorb incident Sunlight. Thin film technology based solar cells use different thin-film technologies (PVD, CVD, Plasma-based, etc.) to sequentially deposit the required thin films of ~ 1–10 μm thickness in a vacuum on different substrates (e.g. glass, polymer, metal, etc.) over large areas with integrated module manufacturing by scribing the layers for interconnections [16].

The structure of a-Si solar cell comprised of p-doped-intrinsic-n-doped (p-i-n) layers. Such a-Si cells exhibited the best photoconversion efficiency of 10.1% [17], but on exposure to Sun light, significant losses are observed in power-conversion efficiencies [18]. To increase efficiency and better stability, thin layers of photoactive material are used. These thin layers hinder the absorption of Sun light and thus reduces the photoconversion efficiency [19]. The bandgap of CdTe is close to ideal bandgap 1.48 eV and usually forms p-n junction solar cell by CdTe deposition on cadmium sulfide (CdS). Demonstration of 21% photoconversion efficiency (PCE) of CdTe solar cells, and 17% with CdTe solar module, by First Solar Inc. U.S.A., has kept the research and commercial interest in this technology alive. The addition of gallium to copper indium diselenide (CIS) results in a recordable efficiency of 21.7% with excellent stability [20]. The CIGS solar module has achieved 16.5% efficiency [21]. The CIGS module made with a cadmium-free buffer has recorded a photoconversion efficiency of 13.5% [22]. Among thin-film photovoltaics, CIGS based solar cells are promising.

GaAs, GaInAsP, GaAlAs, InAs, InP and InSb materials belong to the III-V group of the Periodic Table. Since these materials and alloys can be prepared easily, they lend themselves to the fabrication of monolithic multilayer tandems having solar cells with absorbers operating in different wavelengths of the solar spectrum. In this way, the solar spectrum can be captured by the combination to produce a high-efficiency device. Since these GaAs, GaInAsP, GaAlAs, InAs, InP, and InSb materials were are limited to space and concentrated PV [23]. GaAs has achieved 29.1% PCE as a single junction cell [24]. GaInP/GaAs/GaInAs multi-junction solar cells have the highest 46% PCE [37].

In comparison with first-generation solar cells, the absorption of inident Sun light in second-generation solar cells is far better. Second-generation solar cells have shown efficiencies of 15–20% [25,26]. Poor charge transport is a limiting factor in second-generation solar cells. This inhibits the commercialization of second-generation photovoltaics and led to investigate in new generation PV technologies.

2.3. Emerging photovoltaics or third generation

To avoid the disadvantages of first and second-generation solar cells, researchers started working on a new generation of solar cells known as third-generation or emerging photovoltaics. Emerging photovoltaics are categorized into:

- Dye-sensitized solar cells (DSSC)
- Bulk heterojunction solar cells (BHJ)
- Quantum dot solar cells (QDSSC)
- Perovskite solar cells

These emergent photovoltaics offer several advantages such as low-cost materials, simple processes, abundant and printable on both flexible and non-flexible substrates in the fabrication of solar cells. In DSSC, organic and inorganic-organic dye molecules are used as sensitizers [27]. But in quantum dot solar cells, inorganic quantum dots act as sensitizers and due to the tunable nature of the bandgap, quantum dots offer several advantages over dye molecules but the difficulty of sensitization and selection of efficient electrolyte without the degradation of the quantum dots was a big limitation [28]. In BHJ, conjugated conductive polymers act as donor materials and carbon derivatives such as C_{60} act as acceptor materials [29]. The main disadvantages of BHJ are moisture and ambient light, which can kill the performance of the cell [30]. Recently, CZTS and perovskite solar cells are being under investigation where CZTS solar cells exhibited an efficiency of 12.6% [31], and perovskite solar cells exhibited an efficiency of 23.3% [32]. Among the third generation, DSSC is almost on the verge of commercialization and these can be manufacture both on rigid and flexible substrates.

2.3.1. Dye-sensitized solar cells

The architecture of DSSC contains a mesoporous wide bandgap semiconductor material (typically TiO_2) sensitize a monolayer of dye and a liquid electrolyte with an electrocatalytic platinum counter electrode. In DSSC, TiO_2 acts as a scaffolding layer for dye molecules and also facilitates the charge collection and conduction. The main features of TiO_2 are it is low-cost, abundant, stable and photoactive. Recent developments of ruthenium-based dye molecules are focussed on molecular engineering due to their excellent stability. The N719 is the best charge transfer sensitizer and light absorber and its chemical name are Cis-Di-(thiocyanato) bis (2.2′-bipyridyl)-4,4′-dicarboxylate) ruthenium (II) [33]. The activity of N719 (red dye) is unmatched by any other dye molecules. After a few years, the performance of the new dye called black dye was comparable with red dye [34]. Along with natural dyes, new dyes were designed to achieve high efficiencies [35]. Most of the ruthenium and organic dye molecules have limited absorption in the solar spectrum and form aggregation of dye molecules. In DSSC, the redox iodide/triiodide is commonly used electrolyte is which is volatile, photoreactive and highly corrosive, reacts with the counter electrode and polymeric sealing materials

[36]. As a result, it affects the durability and long term performance.

2.4. Current status of different PV technologies

Since 1980, the efficiency chart of different types of solar cells are released by the National Renewable Energy Laboratory (NREL, USA), and the chart is shown in Fig. 2 [37]. The current research is focussed on the improvement of the device performances by reducing the manufacturing cost. In Fig. 3. the current best laboratory efficiency of solar cell Vs best laboratory module efficiency of different types of all photovoltaic technologies is shown.

2.5. Current market share of different photovoltaic technologies

Crystalline silicon (mono-Si and multi Si) accounts for ~89% of the world-wide PV market share (Fig. 4) while thin-film technologies have the rest. Currently, among the thin-film technologies a-Si, CIGS, CdTe shares are 4%, 1% and 6% [39].

2.6. Cost of PV module

The progression of the PV module's cost from 1992 to 2014 is shown in Fig. 5 [40]. In 1992 it was 5.75 $ Watt^{-1} and the cost of module has decreased year by year until 2000. Then the cost of PV module has increased due to the shortage of the silicon supply until 2008. This situation made the community think about alternative CdTe and CIGS thin-film PV technologies and, as a result, low cost, flexible and lightweight made technologies more attractive. After the entry of Chinese manufacturers into the PV market, the cost of the PV module decreased significantly. A further decrease in the PV module cost will require a solar cell efficiency enhancement with little or no increase in the manufacturing costs.

3. DSSC structure and components

In Fig. 6. The schematic representation of a DSSC device is shown. The DSSC contains semiconductor metal oxide sensitized

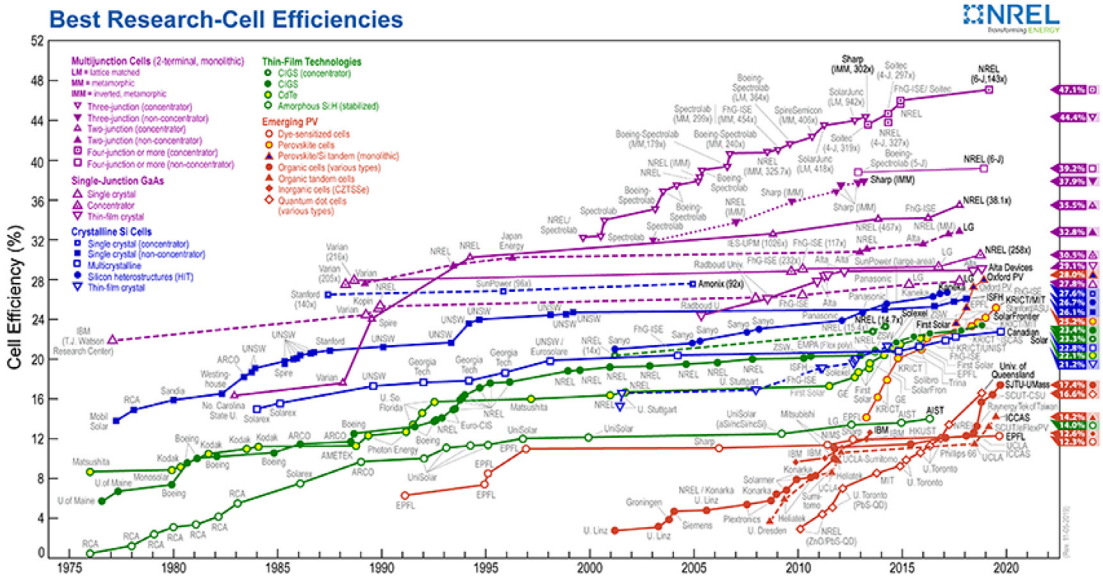

Fig. 2. Year-wise efficiency of different PV technologies. Reproduced with permission from Ref. [38].

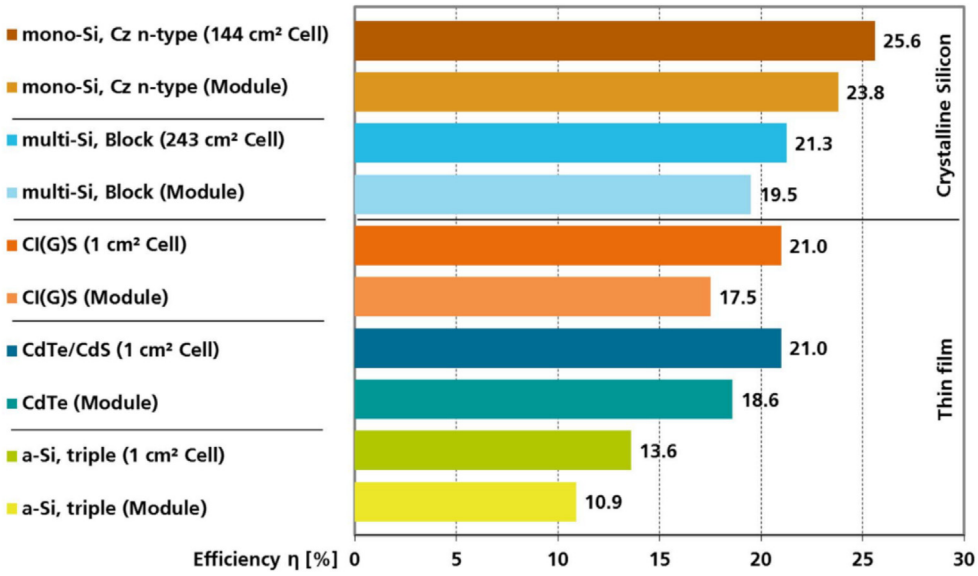

Fig. 3. Best laboratory cells vs best laboratory modules efficiency of different photovoltaic technologies. Reproduced with permission from Ref. [38].

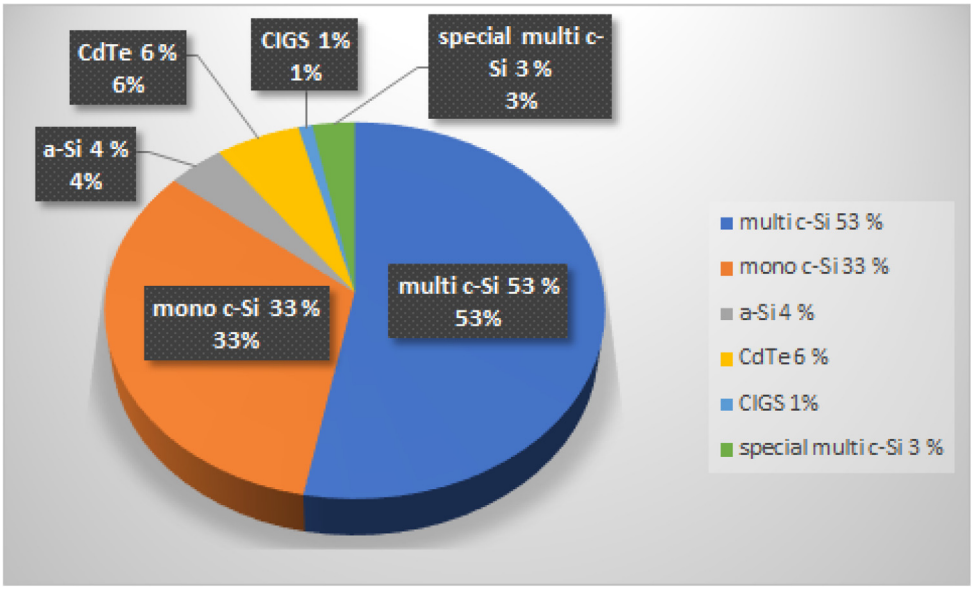

Fig. 4. Current market share of different photovoltaic technologies.

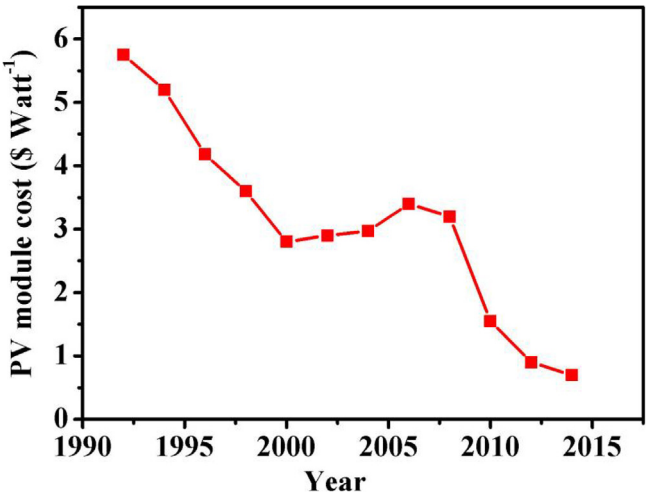

Fig. 5. Year by year cost of the solar module.

with dye molecules termed as photoanode sandwiched with a counter electrode made with a conductive catalyst and filled with liquid redox electrolyte. The working mechanism of the DSSC is shown below

The photoanode is prepared on transparent conductive oxide (TCO) glass substrates with wide bandgap materials with a porous nature where porosity [41] is the measure of empty spaces in the material. The porous nature of the material thus allows the diffusion of dye molecules and facilitates in sensitization. The photoelectrode absorbs lightand generated photons. The photoanode is comprised of nanoparticles to increase anchoring of more dye molecules. Anchoring of more dye molecules results in more absorption of light thus more photocurrent generation. The platinum thin film acts as a counter electrode and prepared on the TCO glass substrate and acts as a counter electrode. The main role of the catalyst was to diffuse the charge carriers into the liquid electrolyte. Another important feature was that the catalyst should be conductive.

The liquid redox electrolyte is penetrated over the photoelectrode and conducts the hole carriers and regeneration of the dye molecules, thus continues the generation of photocurrent. A thermoplastic polymer is used to seal the device by placing between the counter electrode and photoanode to avoid leakage of liquid electrolyte. The components of the device are explained below;

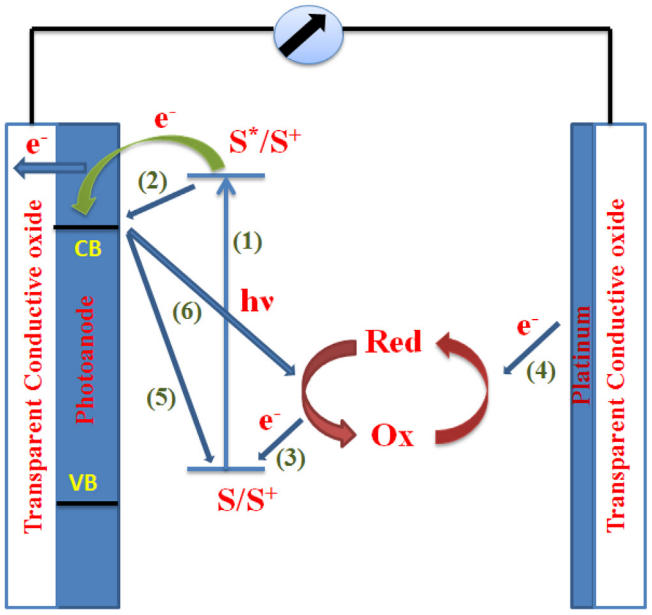

Fig. 6. Schematic representation of DSSC. Reproduced with permission from Ref. [40].

3.1. TCO substrates

TCO substrates are used to prepare the photoelectrode and counter electrode for the device assembly. It acts as a support for the photoanode material (e.g. TiO_2 nanoparticles) and counter electrode catalyst (e.g. platinum). Chemical vapor deposition (CVD) or sputtering techniques are used to deposit TCOs [42,43]. The TCOs prepared by sputtering are flat and need an additional step of chemical wet etching to achieve nanotexture for better light scattering properties and surface adhesion. The TCOs deposited by CVD technology has additional advantages compared to sputtering technology. This process is easily scalable and high deposition

rates with good surface texture. In the last thirty years, many TCOs are developed, but among them, the best are tin-doped indium oxide (ITO) and fluoride doped tin oxide (FTO). For DSSC, FTO substrates are the best choice when compared with ITO due to low cost and it being highly stable up to 550 °C, but FTO has lower optical transparency and electrical conductivity than ITO.

3.2. Photoanodes

Wide bandgap ($E_g \geq 3$ eV) semiconductors oxides are used in the fabrication of photoanodes. These metal oxides absorb most of the incident sunlight, stable to photo-corrosion and optical excitation across the bandgap [44]. Titanium dioxide (TiO_2) is widely investigated photoanode materials for DSSC due to its low cost, stability, catalytic activity and easy to prepare [45]. TiO_2 occurs in four polymorphs. They are anatase [46], rutile [47], brookite [48], and TiO_2(B) [49]. Among them, rutile is the most stable phase and other three are metastable and can be transformed into rutile in the presence of high temperature [50]. Among anatase and rutile, the former has high photocatalytic activity and its electron mobility is 40 times more than rutile [51]. The bandgap of TiO_2 is 3.37 eV and the LUMO energy levels of many dyes lies slightly above the conduction band edge of the TiO_2 and thus facilitates the injection of electrons. The good electrostatic shielding of the injected electrons from the excited dye molecules is due to the high dielectric constant of TiO_2 (ε = 80 for anatase phase). The important features of TiO_2 are non-toxic, low cost and readily available. It is the main constituent of paints and cosmetic products [52].

In DSSC, the photoelectrode is made mostly using mesoporous TiO_2 nanoparticles with a surface area of 50–250 m^2/g. On TCO substrate, the TiO_2 film is coated either by the doctor blade or screen printing method followed by high-temperature treatment to remove organic binders thereby achieving pure TiO_2 film and in turn improves the inter-particle necking between the TiO_2 nanoparticles [53]. Transparent TiO_2 paste is made with nanoparticles of size $\leq$ 20 nm and coated on a TCO substrate initially. Then light scattering paste, which is made with nanoparticles of size 400 nm, is coated on transparent layers of TiO_2 films. Different morphologies such as aerogels [54], mesoporous/nanoporous nanoparticles [55] nanowires [56], nanorods [57], nanobelts [58], nanotubes [59] and hierarchical structures [60], are becoming popular.

Apart from TiO_2, other metal oxides and composite materials such as Au-TiO_2 [61], ZnO [62], Ag_20-ZnO [63], Nb_2O_5 [64], SnO_2 [65], WO_3 [66], Fe_2O_3 [67], are studied as photoanode material. Among them, ZnO is considered as the best alternative to TiO_2 in the fabrication of photoanode for DSSC. The bandgap of the ZnO is 3.3 eV and the energy levels of the conduction band edge lies at the same level of TiO_2. The mobility and carrier lifetime of electrons in ZnO is higher than TiO_2 which is an important feature of DSSC. The synthesis of ZnO is very easy and the growth of different morphologies like nanoparticles, nanowires nanorods, nanotubes, tetrapods is easy. The current state of photoconversion efficiency of DSSC based on ZnO photoanode is 8.0% [68]. But ZnO dissolves in iodide/triiodide electrolyte and form Zn^{2+} ions and thus decreases the efficiency. To overcome the limitations of ZnO in the presence of corrosive redox iodide/triiodide electrolyte, layered double hydroxide is studied as photoanode materials for DSSC [69,70]. There are still options for new structures/materials/architecture for the excellent performance of the DSSC.

3.3. Sensitizers

The dye molecules are also known as sensitizers and play a significant role in the DSSC. These sensitizers absorb sunlight and generate excitons where electrons are injected from the LUMO level into the conduction band of the photoanode and the holes are injected from HOMO level into the redox electrolyte. The amount of absorption of photons by sensitizers dictates the photoconversion efficiency. The photoconversion efficiencies of the different sensitizers are shown in Table 1.

3.4. Counter electrodes

The catalyst is coated on the TCO substrates which ensure the catalytic activity of electron toward the tri-iodide reduction and charge transfer kinetics of electrons at the cathode. Platinum and carbon-related materials are commonly used catalyst materials for the applicatio of counter electrodes. Among them, platinum acts as a better catalyst and its electrical conductivity are high. The platinum counter electrode is prepared by spin coating, sputtering and vapor deposition and electrochemical methods [85]. The cost of platinum is the limiting factor for the commercialization of DSSC. Graphite is considered one of the alternatives to platinum due to its low cost and easy preparation [86]. But the efficiencies of the graphite-based DSSC are poor in comparison with the platinum-based DSSC. Other materials such as graphene and graphene-related materials [87], conductive polymers such as PEDOT:PSS [88], chalcogenides [89–91], and p-type metal oxides [92], are tested as counter electrodes and but platinum is still the leader among all.

Table 1
States of the art of different dye molecules investigated in DSSC.

S.No	Dye	V_{oc}(V)	J_{sc} (mA/cm^2)	FF (%)	η((%)	Area (cm^2)	Electrolyte	Ref
1	ADEKA-1/ LEG4	1.05	18.27	77.1	14.3	–	Co(II)/Co(III)	[6]
2	N719	0.79	15.6	74.0	9.12	0.16	I^-/I_3^-	[53]
3	SM315	0.91	18.1	78.0	13.0	0.28	Co(II)/Co(III)	[71]
4	N3	0.72	18.2	73.0	10	–	I^-/I_3^-	[72]
5	Black dye	0.74	20.86	72.2	11.1	0.22	I^-/I_3^-	[73]
6	SA246	0.84	14.55	74.7	9.4	–	Co(II)/Co(III)	[74]
7	YD2-o-C8	0.93	17.05	77.9	12.29	–	Co(II)/Co(III)	[75]
8	HD-8	0.68	16.96	68.0	7.9	0.18	Iodolyte AN-50	[76]
9	PYR–Por–MA	0.52	8.19	73.2	3.14	0.25	I^-/I_3^-	[77]
10	JF419	0.84	16.2	76.0	10. 3	–	Co(II)/Co(III)	[78]
11	TFRS-4	0.73	18.7	73.0	10.2	0.16	I^-/I_3^-	[79]
12	RD-18	0.72	18.93	72.0	10.0	0.16	I^-/I_3^-	[80]
13	C106	0.76	19.78	78.0	11.7	0.16	I^-/I_3^-	[81]
14	CYC-B11	0.70	18. 3	73.0	9.4	0.16	Z946	[82]
15	C218	0.76	14.8	77.0	8.6	–	Co(II)/Co(III)	[87]
16	TTAR-b8	0.81	17.54	72.0	10.2	–	I^-/I_3^-	[83]
17	D205	0.71	18.68	70.7	9.4	–	I^-/I_3^-	[84]

3.5. Electrolytes

The major role of redox electrolyte in DSSC is to inject the holes into the electrolyte and to regenerate of the oxidized sensitizers

Any electrolyte employed in the DSSC must fulfil the following requirements [93].

- The electrolyte should exhibit thermal, chemical, optical and electrochemical stability and must prevent dye degradation.
- The hole carriers must be injected into the electrolyte and regenerate the oxidized dye molecules to the ground state.
- The absorption spectrum of the electrolyte should not overlap with that of the dye and the visible spectrum.

Based on the viscosity and constituent's components, the nature of electrolyte is classified into solid, liquid and quasi. In DSSC, redox couple iodide/triiodide (I^-/I_3^-) is widely investigated due to its unique slow recombination rates [94]. Triiodide ions absorb the visible light and also react with the injected electrons. Optimization of iodide and triiodide ions is necessary for better performance. Due to corrosive nature of I^-/I_3^- electrolyte, research leads in the preparation of new redox electrolytes such as $SCN^-/(SCN)_3^-$, $SeCN^-/(SeCN)_3^-$, and Br^-/Br_3^- [95–97]. The performances of these electrolytes are promising but they have poor chemical stability. Copper and cobalt-based coordination compounds can act as redox couples [98,99]. Among them, cobalt-based coordination compounds exhibited excellent photoconversion performance. The current state of the art of DSSC based on cobalt-based redox couple is 14.3% achieved with modified Y123 dye [85]. The important features of the cobalt-based redox couple were non-corrosive, transparent and non-volatile.

4. Recent developments in DSSC

4.1. Optimization of the room temperature binder-free TiO_2 paste for high-efficiency flexible polymer DSSC

The TiO_2 paste is successfully prepared without using binder molecules at room temperature. The doctor blade method is adopted in the preparation of TiO_2 films on flexible polymer PEN substrates. The devices prepared with these films exhibited excellent photovoltaic parameters. It was observed that; longer stirring hours do not improve the photoconversion efficiencies. Memory effects of the TiO_2 paste were checked with 50 days old paste and the results were promising indicating the durability and stability of the TiO_2 paste. The DSSC prepared with 8 h stirring paste and with flash annealing resulted in photoconversion efficiency of 4.2%. Better results are possible with the addition of a blocking layer and high-temperature resistance flexible polymer substrates [100].

4.2. Binder free titania-graphene quantum dots paste for flexible DSSCs

Graphene oxide is synthesized using the modified Hummer's method. Graphene quantum dots were successfully synthesized using reduced graphene oxide by the electrochemical cyclic voltammetry technique. The graphene quantum dots solution was added to the optimized binder-free TiO_2 paste and GQD-TiO_2 paste was prepared. The GQD-TiO_2 films were prepared with optimized conditions and GQD-TiO_2 hybrids-base DSSC device exhibited a photoconversion efficiency (η) of 4.43% with V_{oc} = 0.73 V, J_{sc} = 11.54 mA/cm^2 and FF = 52.7%. To further improve the better performance of GQD-TiO_2 films in DSSCs is possible with a higher concentration of GQDs in the paste preparation [101].

4.3. Screen printed graphene oxide (GO) films as an efficient counter electrode in DSSC

α-terpineol is employed in the preparation of GO paste and the GO films are made by screen printing on FTO substrates. The cells assembled with these films resulted in poor photovoltaic parameters due to the poor adhesion of GO films. Ethylcellulose binder molecules are added in the paste preparation to improve the adhesion of GO films. The GO films are annealed at 500 °C to remove the binder molecules. The GO films made with the paste containing ethyl cellulose showed a drastic improvement in the adhesion. The DSSC made with these films showed better photoconversion efficiency. The photoconversion efficiency improved from 0.3% to 5.58%. Due to the good adhesion of the GO films, an increment is observed in the short circuit current and fill factor which in turn results in good photoconversion efficiency [89].

4.4. Investigation of screen printed tin selenide counter electrode in DSSCs

In the synthesis of tin selenide (SnSe), equimolar amounts of selenium are tin powder is grounded stoichiometrically and subjected to the solid-state reaction in a closed container. SnSe paste is prepared with optimized conditions. The screen printing method is employed in the preparation of SnSe films on FTO substrates and DSSCs are assembled with SnSe-CE. The photoconversion parameters are dependent on the SnSe thickness. However, increasing the thickness beyond SnSe-7L, resulted in decreasing photoconversion parameters. Further improvement of the device performance can be achieved with additional treatments such as annealing the SnSe films in selenium environment and other methods of film preparation like electrodeposition spray deposition techniques [91].

4.5. Phenanthroline-based ruthenium complex polymeric materials as additives in redox electrolyte

The phenanthroline-based ruthenium complex monomer and its polymers are used as additives molecules in the preparation of redox iodide/triiodide electrolyte. when compared linear polymers, the armed polymers exhibited higher J_{sc} which resulted in higher photoconversion efficiencies. The incorporation of these phenanthroline-based ruthenium complex polymers in the redox electrolyte increases longevity and also an important aspect of the commercialization of DSSC [102].

5. Electrical characteristics parameters

Under illumination, the solar cells are testified with photovoltaic parameters such as the J_{sc}, V_{oc} FF and PCE. The J-V characteristics of photovoltaic cells are validated with photovoltaic parameters.

5.1. Open-circuit voltage

To annihilate the current generated during illumination, a bias voltage (open-circuit voltage (V_{oc})) is applied to solar cells. Under illumination, the external current (J = 0) doesn't flow at the V_{oc}. In DSSC, the V_{oc} depends on the work function of the Fermi energy of the photoanode and electrolyte [103]. Owing to the recombination of charge carriers, the V_{oc} is a bit low determined experimentally. To achieve the theoretical limit is possible when all recombination processes are minimized. All charge carriers will undergo recombination within the photoactive layer at open-circuit conditions. It is observed that it is difficult to avoid recombination processes due to the thermodynamic

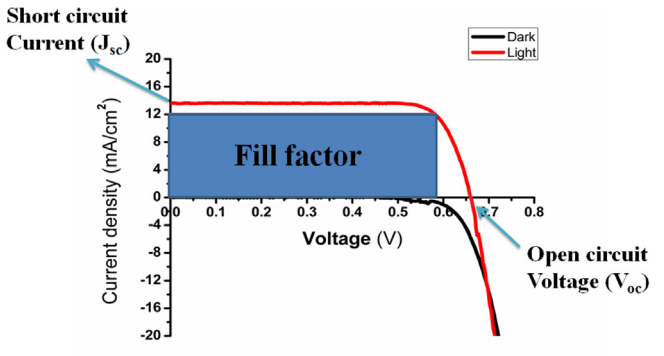

Fig. 7. Schematic representation of the J-V characteristic curve of DSSC. Reproduced with permission from Ref. [106].

considerations of the balance between the recombination of photo-generation and charge carriers [104].

5.2. Short- circuit current density (J_{sc})

At applied zero bias, the current density generated in a solar cell is termed as J_{sc}. The build-in-potential is generated due to exciton dissociation and charge transport. The J_{sc} of a DSSC is dependent on incident light and generation of excitons. Secondly, a wide absorption spectrum of the photoactive layer leads to harvest more excitons within the terrestrial solar spectrum which leads to maximum J_{sc} of the DSSC. The charge carrier mobility of the active layer determines the J_{sc} of solar cell [105].

5.3. Fill factor (FF%)

The J-V characteristics of DSSC are shown in Fig. 7. The main objective of a solar cell is the conversion of sun light into electricity. From the J-V curve, we can calculate the P_{max} where P_{max} represents the maximum deliverable power. The fill factor of the DSSC is calculated using the expression below;

$$\mathbf{FF}\% = \frac{\mathbf{P_{max}}}{\mathbf{J_{sc}} \times \mathbf{V_{oc}}} = \frac{\mathbf{J_{max}} \times \mathbf{V_{max}}}{\mathbf{J_{sc}} \times \mathbf{V_{oc}}} \quad (1)$$

The diode characteristics of solar cells can be measured with the FF. For an ideal diode, the FF must be unity. As the higher FF, the diode will be more ideal. In DSSC, due to the losses occurring by recombination and transport, the FF found between 0.6 and 0.85 [107]. In solar cells, it is observed that shunt and series resistance acts as limiting factors [108]. Large shunt resistance and low series resistance in solar cells lead to high fill factor FF.

5.4. Power conversion efficiency (η)

The efficiency of a DSSC is defined as the ratio between the delivered power (P_{max}) and the incident light power (P_{in}). The photoconversion efficiency of the solar cell is calculated using the expression below;

$$\eta = \frac{\mathbf{P_{max}}}{\mathbf{P_{in}}} = \frac{\mathbf{J_{sc}} \times \mathbf{V_{oc}} \times \mathbf{FF}}{\mathbf{P_{in}}} \quad (2)$$

The η tells about the output power of the DSSC and gives an idea about the conversion of light into electricity and photovoltaic parameters.

5.5. Dark current

In dark conditions, the current passing through the diode is termed as dark current. The recombination of charge carriers or any kind of surface leakage in the depletion region is the basis of the dark current generation and is as ideal diode current [109]. The generation of the potential difference between the terminals of the solar cell is caused when a forward bias load is applied. This potential difference generates a current which acts in the opposite direction to the photocurrent, and the net current is reduced from its short circuit value. This reverse current is usually called dark current in analogy with the current I_{dark} (V) which flows across the device under an applied voltage in the dark. In dark conditions, solar cells acts like a diode which accepts a larger current under forward bias (V > 0) on compared to reverse bias (V < 0). This behaviour is a characteristic feature of solar cells since asymmetry is required to achieve charge separation.

5.6. Standard test conditions

The test conditions to calculate the photovoltaic parameters of the DSSC have been designed to obtain comparable and meaningful values because temperature, irradiation, humidity and illumination intensity dictate the photovoltaic parameters. These device test conditions are based on Sun's emission spectrum and spectral distribution on a clear sunny day with a radiant intensity of 100 mW/cm^2 received on a tilted plane surface with an angle of incidence of 48.2°. This Sun's emission spectrum also counts for a model atmosphere "Air Mass 1.5 Global" (AM1.5G, IEC 904–3) spectrum containing specified concentrations of moisture, carbon dioxide, and aerosol.

6. Conclusions

In summary, this report is study focussed on realising DSSC with cost-effective, earth-abundant materials, using processes that could be easily transferable on an industrial scale. Recently, the following works were developed for the development of DSSC. Binder free TiO_2 paste preparation is developed for flexible polymer DSSCs. To enhance efficiency, graphene quantum dots were used in the preparation of binder-free TiO_2 paste. The performance of the flexible polymer devices could be improved by the addition of a blocking layer on the polymer flexible substrates. A high-temperature treatment can also improve the performance but temperature resistant polymer films are needed for this kind of temperature treatment. Increasing the amount of GQDs in the binder-free TiO_2 paste can enhance the performance of the DSSCs. Earth-abundant, low cost and non-toxic SnSe and GO films are prepared by screen printing method and used as counter electrodes in DSSC. Screen printed SnSe films on a large area on FTO substrates followed by the sulphurisation/selenization can be used as an efficient CE for the DSSC at the industrial scale. GO and SnSe CE could be best suitable for the DSSC assembled with monolithic architecture. To further boost the efficiency of GO and SnSe CE, the films could be prepared with other cost-effective methods such as spray deposition or electrodeposition and the addition of other materials such as conductive polymers, metal nanoparticles and carbon materials. Phenanthroline-based ruthenium complex polymeric materials act as additives in redox iodide/troiodide electrolyte. This ruthenium-based polymers increases the lifetime of the electrolyte which is one of the important features for the commercialization of DSSC.

Declaration of Competing Interest

The authors declare that they have no known competing financial interests or personal relationships that could have appeared to influence the work reported in this paper.

Acknowledgments

The authors thank the EPRSC-DST APEX consortium grant number EP/H040218/1 and "International mobilities for research activities of the University of Hradec Králové", CZ.02.2.69/0.0/0.0/16_027/0008487 for the financial support.

References

[1] BP Statistical Review of World Energy June 2010. BP, London, 2010.
[2] G. Reddy, K. Devulapally, N. Islavath, L. Giribabu, Chem. Rec. 19 (2019) 2157–2177.
[3] W. Shockley, H.J. Queisser, J. Appl. Phys. 32 (1961) 510.
[4] B. O'Regan, M. Gratzel, Nature 353 (1991) 737.
[5] K. Kakiage, Y. Aoyama, T. Yano, K. Oya, J.-I. Fujisawa, M. Hanaya, Chem. Commun. 51 (2015) 15894–15897.
[6] Mike B. Roberts, Anna Bruce, Iain MacGill, Sol. Energy 193 (2019) 372–386.
[7] A. Blakers, K. Weber, V. Everett, Chem. Aust. 72 (2005) 9.
[8] http://www.electronics-tutorials.ws/diode/diode_3.html.
[9] M.A. Green, K. Emery, Y. Hishikawa, W. Warta, E.D. Dunlop, Prog. Photovolt: Res. Appl. 23 (2015) 1.
[10] F.C. Marques, A.D. Soares Cortes, P.R. Mei, Silicon 11 (2019) 77–83.
[11] Goksin Kavlak, James McNerney, Jessika E. Trancik, Energy Policy 123 (2018) 700–710.
[12] L.C. Rogers, W.C. O'Mara, R.B. Herring, and L.P. Hunt, Handbook of Semiconductor Silicon Technology, Noyes Publications, New Jersey, USA (1990).
[13] W. Wettling, Sol. Energy Mater. Sol. Cell 38 (1995) 487.
[14] F. Antony, C. Durschner, K-H. Remmers, Photovoltaics for professional, Solarpraxis AG, London, 2007.
[15] N.M. Kumar, K. Sudhakar, M. Samykano, Int. J. Ambient Energy 40 (2019) 434–443.
[16] T. Muñoz-Rojas, A. Maindron, F. Esteve, J.C.S. Piallat, J.-M. Kools, Materials Today Chemistry 12 (2019) 96–120.
[17] J. Seo, W.J. Kim, S.J. Kim, K.-S. Lee, A.N. Cartwright, P.N. Prasad, Appl. Phys. Lett. 94 (2009) 133302.
[18] F.U. Hamelmann, J.A. Weicht, G. Behrens, J. Phys. Conf. Ser. 682 (2016) 012002.
[19] F. Meillaud, M. Boccard, G. Bugnon, M. Despeisse, S. Hänni, F.-J. Haug, J. Persoz, J.-W. Schüttauf, M. Stuckelberger, C. Ballif, Mater. Today 18 (2015) 378.
[20] P. Jackson, D. Hariskos, R. Wuerz, O. Kiowski, A. Bauer, Th.M. Friedlmeier, M. Powalla, Phys. Status Solidi RRL 9 (2015) 28.
[21] Sean Y., Kwang-Ming L., Wen-Chin L., Wen-Shun L., Chia-Hsiang C., Jyh-Lih W., Chi-Yu C., Chung-Hsien W., Yu-Lun S., Henry L., Chin-Hsiang C., Liham C., IEEE 42nd Photovoltaic Specialist Conference (PVSC), 2015.
[22] Y. Tanaka, N. Akema, T. Morishita, D. Okumura, K. Kushiya, Conf. Proceedings, 17th EC photovoltaic solar energy conference, Munich, October, 2001 989.
[23] N.A. Pakhanov, V.M. Andreev, M.Z. Shvarts, O.P. Pchelyakov, Optoelectron. Instrument. Proc. 54 (2018) 187–202.
[24] M.A. Green, K. Emery, Y. Hishikawa, W. Warta, E.D. Dunlop, Solar cell efficiency tables (Version 53), Prog. Photovolt: Res. Appl. 27 (2019) 3–12.
[25] R. Schropp, M. Zeman (Eds.), Amorphous and Microcystalline Silicon Solar Cells: Modelling, Materials and Device Technology" Kluwer, Boston, 1998.
[26] R. Noufi, K. Zweibel (Eds.), High-Efficiency CdTe and CIGS Thin-Film Solar Cells: Highlights and Challenges," IEEE 4th World Conf. on Photovoltaic Energy Conversion, 2006, 1, 317.
[27] N. Chadwick, D.K. Kumar, A. Ivaturi, B.A. Grew, H.M. Upadhyaya, L.J. Yellowlees, N. Robertson, Eur. J. Inorg. Chem. 2015 (2015) 4878–4884.
[28] E. Akman, Y. Altintas, M. Gulen, M. Yilmaz, E. Mutlugun, S. Sonmezoglu, Renewable Energy 145 (2020) 2192–2200.
[29] M. Riede, T. Mueller, W. Tress, R. Schueppel and K. Leo, Nanotechnology, 2008, 424001; B. P. Rand, J. Genoe, P. Heremans, J. Poortmans, Prog. Photovoltaics, 2007, 15, 659; B. C. Thompson, J. M. J. Frechet, Angew. Chem., Int. Ed. 2008, 47, 58.
[30] O.A. Abdulrazzaq, V. Saini, S. Bourdo, E. Dervishi, A.S. Biris, Part. Sci. Technol. 31 (2013) 427.
[31] W. Wang, M.T. Winkler, O. Gunawan, T. Gokmen, T.K. Todorov, Y. Zhu, D.B. Mitzi, Adv. Energy Mater. 4 (2013) 1301465.
[32] Q. Jiang, Y. Zhao, X. Zhang, X. Yang, Y. Chen, Z. Chu, Q. Ye, X. Li, Z. Yin, J. You, Nat. Photonics 13 (2019) 460–466.
[33] S. Nakade, W. Kubo, Y. Saito, T. Kanzaki, T. Kitamura, T.Y. Wada, S. Yanagida, J. Phys. Chem. B (2003) 107.
[34] M.K. Nazeeruddin, A. Kay, I. Rodicio, R. Humphrey-Baker, E. Muller, P. Liska, N. Vlachopoulos, M.J. Gratzel, Am. Chem. Soc. 115 (1993) 6382.
[35] M. H. Buraidah, L. P. Teo, S. N. F. Yusuf, M. M. Noor, M. Z. Kufian, M. A. Careem, S. R. Majid, R. M. Taha, A. K. Arof, International Journal of Photoenergy, 2011, 11 & S. Kim, J. K. Lee, S. O. Kang, J. Ko, J-H. Yum, S. Fantacci, F. D. Angelis, D. D. Censo, M. K. Nazeeruddin, M. Gratzel, Journal of the American Chemical Society, 2008, 128, 16701.
[36] I. Lee, S. Hwang, H. Kim, Sol. Energy Mater. Sol. Cells 95 (2011) 315.
[37] https://www.nrel.gov/pv/cell-efficiency.html.
[38] M. Green, Solar Cell Efficiency Tables (Version 48), Progress in PV: Research and Applications 2016.
[39] M. Green, Commercial progress and challenges for photovoltaics, Nat Energy 1 (2016) 15015.
[40] C. Anselmi, E. Mosconi, M. Pastore, E. Ronca, F.D. Angelis, Phys. Chem. Chem. Phys. 14 (2012) 15963.
[41] R. Jeba Beula, Devadason Suganthi, A. Abiram, Appl. Phys. A 126 (2020) 223.
[42] M. Tadatsugu, Thin Solid Films 516 (2008) 5822.
[43] F. Kurdesau, G. Khripunov, A.F. da Cunha, M. Kaelin, A.N. Tiwari, J. Non-Cryst. Solids 352 (2006) 1466.
[44] H. Yu, S. Zhang, H. Zhao, B. Xue, P. Liu, G. Will, J. Phys. Chem. C 113 (2009) 16277.
[45] Y. Wang, D.J. Doren, Solid State Commun. 136 (2005) 186.
[46] M. Ojeda, D.K. Kumar, B. Chen, J. Xuan, M.M. Maroto-Valer, D.Y.C. Leung, H. Wang, Chemistry Select 2 (2017) 702–706.
[47] N. Sriharan, N.M. Ganesan, L. MisookKang, T.S. Senthil Kungumadevi, Mater. Lett. 237 (2019) 204–208.
[48] H. Lin, L. Li, M. Zhao, X. Huang, X. Chen, G. Li, R. Yu, J. Am. Chem. Soc. 134 (2012) 8328.
[49] S.F. Shen, M.J. Chang, Y.H. Liu, H.B. Pan, N.S. Chen, Chin. J. Inorg. Chem. 28 (2012) 1099.
[50] D.A.H. Hanaor, Charles C. Sorrell, J. Mater. Sci. 46 (2011) 855.
[51] F. Xiong, L.-L. Yin, F. Li, Z. Wu, Z. Wang, G. Sun, H. Xu, P. Chai, X.-Q. Gong, W. Huang, J. Phys. Chem. C 123 (2019) 24558–24565.
[52] B. Swain, J.R. Park, K.-S. Park, C.G. Lee, Mater. Sci. Eng., C 95 (2019) 95–103.
[53] S. Ito, T.N. Murakami, P. Comte, P. Liska, C. Grätzel, M.K. Nazeeruddin, M. Grätzel, Thin Solid Films 516 (2008) 4613.
[54] Z. Zhao, X. Jiao, D. Chen, J. Mater. Chem. 19 (2009) 3078.
[55] A. Hegazy, N. Kinadjian, B. Sadeghimakki, S. Sivoththaman, N.K. Allam, E, Prouzet, Sol. Energy Mater. Sol. Cells 153 (2016) 108.
[56] M. Munz, M.T. Langridge, K.K. Devarepally, D.C. Cox, P. Patel, N.A. Martin, G. Vargha, V. Stolojan, S. White, R.J. Curry, A.C.S. Appl, Mater. Interfaces 5 (2013) 1197.
[57] Z. Yang, B. Wang, H. Cui, H. An, Y. Pan, J. Zhai, J. Phys. Chem. C 119 (2015) 16905.
[58] Z. Han, J. Zhang, W. Cao, Mater. Lett. 84 (2012) 34.
[59] J.M. Macak, H. Tsuchiya1, A. Ghicov, K. Yasuda, R. Hahn, S. Bauer, P. Schmuki, Current Opinion in Solid State and Materials Science, 2007, 11, 3.
[60] X. Meng, D.-W. Shin, S.M. Yu, J.H. Jung, H.I. Kim, H.M. Lee, Y.-H. Han, V. Bhoraskar, J.-B. Yoo, Cryst. Eng. Comm. 13 (2011) 3021.
[61] T. Solaiyammal, P. Murugakoothan, Green synthesis of Au and the impact of Au on the efficiency of TiO2 based dye sensitized solar cell, Mater. Sci. Energy Technol. 2 (2019) 171–180.
[62] N. Sakai, T. Miyasaka and T. N. Murakami, J. Phys. Chem. C, 2013, 117, 10949 & J. Han, F. Fan, C. Xu, S. Lin, M. Wei, X. Duan and Z. L. Wang, Nanotechnology 2010, 21, 405203.
[63] A.M. Ibraheem, J. Kamalakkannan, Science for Energy Technologies 3 (2019) 183–192.
[64] A. Le Viet, R. Jose, M.V. Reddy, B.V.R. Chowdari, S. Ramakrishna, J. Phys. Chem. C 114 (2010) 21795.
[65] A. Birkel, Y.-G. Lee, D. Koll, X.V. Meerbeek, S. Frank, M. Choi, Y.S. Kang, K. Char, W. Tremel, Energy Environ. Sci. 5 (2012) 5392.
[66] X. Chen, J. Ye, S. Ouyang, T. Kako, Z. Li, Z. Zou, ACS Nano 5 (2011) 4310.
[67] M. Cavasa, R.K. Gupta, A. Al-Ghamdic, Z. H. Gaferc, F. El-Tantawyd, F. Yakuphanoglu, Materials Letters, 2013, 105, 106 & H. Niu, S. Zhang, Q. Ma, S. Qin, L. Wan, J. Xu and S. Miao, RSC Adv., 2013,3, 17228.
[68] Y. He, J. Hua, Y. Xie, Chem. Commun. 51 (2015) 16229.
[69] S. Liu, J. Liu, T. Wang, C. Wang, Z. Ge, J. Liu, X. Hao, N. Du, H. Xiao, Colloids Surf., A 568 (2019) 59–65.
[70] L.J. Foruzin, Z. Rezvani, K. Nejati, Sol. Energy 186 (2019) 106–112.
[71] S. Mathew, A. Yella, P. Gao, R. Humphry-Baker, B.F.E. Curchod, N. Ashari-Astani, I. Tavernelli, U. Rothlisberger, M.K. KhajaNazeeruddin, M. Grätzel, Nat. Chem. 6 (2014) 242.
[72] M. K. Nazeeruddin, A. Kay, 1. Rodicio, R. Humpbry-Baker, E. Miiller, P. Liska, N. Vlachopoulos, and M. Gratzel, J. Am. Chem. Soc. 1993,115, 6382.
[73] Y. Chiba, A. Islam, Y. Watanabe, R. Komiya, N. Koide, L. Han, Jpn. J. Appl. Phys. 45 (2006) 638.
[74] S. Aghazada, P. Gao, A. Yella, G. Marotta, T. Moehl, J. Teuscher, J.-E. Moser, F. De Angelis, M. Gratzel, M.K. Nazeeruddin, Inorg. Chem. 55 (2016) 6653.
[75] A. Yella, H.-W. Lee, H.N. Tsao, C. Yi, A.K. Chandiran, M.K. Nazeeruddin, E.W.-G. Diau, C.-Y. Yeh, S.M. Zakeeruddin, M. Grätzel, Science 334 (2011) 629.
[76] H. Cheema, R. Younts, L. Ogbose, B. Gautam, K. Gundogdu, A. El-Shafeia, Phys. Chem. Chem. Phys. 17 (2015) 2750.
[77] P.S. Reeta, L. Giribabu, S. Senthilarasu, M.-H. Hsu, D.K. Kumar, H.M. Upadhyaya, N. Robertson, T. Hewat, RSC Adv. 4 (2014) 14165.
[78] A. Yella, R. Humphry-Baker, B.F.E. Curchod, N.A. Astani, J. Teuscher, L.E. Polander, S. Mathew, J.-E. Moser, I. Tavernelli, U. Rothlisberger, M. Gratzel, M. K. Nazeeruddin, J. Frey, Chem. Mater. 25 (2013) 2733.
[79] S.-W. Wang, K.-L. Wu, E. Ghadiri, M.G. Lobello, S.-T. Ho, Y. Chi, J.-E. Moser, F.D. Angelis, M. Gratzel, M.K. Nazeeruddin, Chem. Sci. 4 (2013) 2423.
[80] W.-K. Huang, H.-P. Wu, P.-L. Lin, E.W.-G. Diau, J. Phys. Chem. C 117 (2013) 2059.
[81] Q. Yu, Y. Wang, Z. Yi, N. Zu, J. Zhang, M. Zhang, P. Wang, ACS Nano 4 (2010) 6032.

[82] C.-Y. Chen, M. Wang, J.-Y. Li, N. Pootrakulchote, L. Alibabaei, C.-H. Ngocle, J.-D. Decoppet, J.-H. Tsai, C. Gratzel, C.-G. Wu, S.M. Zakeeruddin, M. Gratzel, ACS Nano 3 (2009) 3103.
[83] Y. Ezhumalai, B. Lee, M-S. Fan, B. Harutyunyan, K. Prabakaran, C-P. Lee, S. H. Chang, J-S. Ni, S. Vegiraju, P. Priyanka, Y-W Wu, C-W Liu, S. Yau, J. T. Lin, C-G. Wu, M. J. Bedzyk, R. P. H. Chang, M-C Chen, K-C. Ho and T. J. Marks, J. Mater. Chem. A, 2017, 5, 12310.
[84] S. Ito, H. Miura, S. Uchida, M. Takata, K. Sumioka, P. Liska, P. Comte, P. Pechy, M. Gratzel, Chem. Commun. (2008) 5194.
[85] G. Calogero, P. Calandra, A. Irrera, A. Sinopoli, I. Citro, G.D. Marco, Energy Environ. Sci. 2011 (1838) 4.
[86] M.F. Don, P. Ekanayake, H. Nakajima, A.H. Mahadi, C.M. Lim, A. Atod, Ionics 25 (2019) 5585–5593.
[87] D. Kishore Kumar, S.K. Swami, V. Dutta, B. Chen, N. Bennett, H.M. Upadhyaya, Flat Chem 15 (2019) 100105.
[88] C.-H. Chiang, C.-G. Wu, Org. Electron. 14 (2013) 1769.
[89] D. Kishore Kumar, S.R. Popuri, O.R. Onuoha, J.-W. Bos, B. Chen, N. Bennett, H. M. Upadhyaya, Sol. Energy 190 (2019) 28–33.
[90] S.K. Swami, N. Chaturvedi, A. Kumar, N. Chander, V. Dutta, D.K. Kumar, A. Ivaturi, S. Senthilarasu, H.M. Upadhyaya, Phys. Chem. Chem. Phys. 16 (2014) 23993.
[91] S. Prasad, D. Devaraj, R. Boddula, S. Salla, M.S. AlSalhi, Materials Science for Energy Technologies 2 (2019) 319–328.
[92] H. Wang, W. Wei, Y.H. Hu, Top. Catal. 57 (2014) 607.
[93] J. Cong, X. Yang, Y. Hao, L. Kloo L Sun, RSC Advances 2 (2012) 3625–3629.
[94] M. Wang, C. Gratzel, S.M. Zakeeruddin, M. Gratzel, Energy Environ. Sci. 5 (2012) 9394.
[95] G. Oskam, B.V. Bergeron, G.J. Meyer, P.C. Searson, J. Phys. Chem. B 105 (2001) 6867.
[96] F. Bella, A. Sacco, G.P. Salvador, S. Bianco, E. Tresso, C.F. Pirri, R. Bongiovanni, J. Phys. Chem. C 117 (2013) 20421.
[97] S. Ferrere, A. Zaban, B.A. Gregg, J. Phys. Chem. B 101 (1997) 4490.
[98] Y. Bai, Q. Yu, N. Cai, Y. Wang, M. Zhang, P. Wang, Chem. Commun. 47 (2011) 4376.
[99] A. Yella, H.W. Lee, H.N. Tsao, C. Yi, A.K. Chandiran, M.K. Nazeeruddin, E.W.G. Diau, C.Y. Yeh, S.M. Zakeeruddin, M. Gratzel, Science 334 (2011) 629.
[100] D.K. Kumar, M.-H. Hsu, A. Ivaturi, B. Chen, N. Bennett, H.M. Upadhyaya, Flexible Printed Electron. 4 (2019) 015007.
[101] D. Kishore Kumar, D. Suazo-Davila, N.P. Desirée García-Torres, Min-Hung Hsu Cook, A. Ivaturi, A.A. Martí, C.R. Cabrera, H.M. Upadhyaya, Electrochim. Acta 305 (2019) 278–284.
[102] J. Gopinath, R. Kumar, C. Balasubramanyam, V. Santosh, S.K. Swami, D. KishoreKumar, S.K. Gupta, V. Dutta, K.R. Reddy, V. Sadhu, A.V. SeshaSainath, T.M. Aminabhavi, Chem. Eng. J. 358 (2019) 1166–1175.
[103] J. Maçaira, L. Andrade, A. Mendes, RSC Adv. 4 (2014) 2830.
[104] V. Dyakonov, Physica E 14 (2002) 53.
[105] S. Shin, J.H. Seok, B.J. Kang, W. Yin, S.J. Lee, J.H. Noh, T.K. Ahn, F. Rotermund, I. S. Cho, S. Il Seok, Energy Environ. Sci. 12 (2019) 958–964.
[106] L.L. Tobin, T. O'Reilly, D. Zerulla, J.T. Sheridan, Optik – Int. J. Light Electron Opt. 122 (2011) 1225.
[107] N. Sharifi, F. Tajabadi, N. Taghavinia, ChemPhysChem 15 (2014) 3902.
[108] A. Onno, C. Chen, P. Koswatta, M. Boccard, Z.C. Holman, J. Appl. Phys. 126 (2019) 183103.
[109] J. H. Rhee, C-C. Chung and E. W-G. Diau, NPG Asia Materials, 2013, 5, e68.